

1 **Reversible metamorphosis in a bacterium**

2

3 Karina Ramijan¹, Joost Willems¹, Eveline Ultee¹, A. Joeri Wondergem², Anne van
4 der Meij¹, Ariane Briegel¹, Doris Heinrich², Gilles P. van Wezel¹, and
5 Dennis Claessen^{1,#}

6

7 ¹ Molecular Biotechnology, Institute Biology Leiden, Leiden University. ² Leiden
8 Institute of Physics (LION), Huygens-Kamerlingh Onnes Laboratory. Leiden
9 University.

10

11

12

13 # To whom correspondence should be addressed:

14 E-mail: D.Claessen@biology.leidenuniv.nl

15 Tel: +31 (0)71 527 5052

16

17 Keywords: reversible metamorphosis, cell wall synthesis, cell division, origin of life,

18 L-forms, synthetic biology

19

20 **ABSTRACT**

21 The cell wall is a shape-defining and protective structure that envelops virtually all
22 bacteria. Wall-less variants, called L-forms, have been generated in laboratories for
23 many decades under highly specialized conditions, invariably aimed at interrupting
24 cell wall synthesis. As such, the relevance of these cells has remained obscure. Here
25 we show that the filamentous actinomycete *Kitasatospora viridifaciens* has the natural
26 ability to switch between a wall-less state and the canonical mycelial mode-of-growth.
27 We show that this organism thrives in a cell wall-less form, and identify the polar
28 growth determinant DivIVA as an essential regulator required for reversible
29 metamorphosis. This is the first report of a reversible metamorphosis in a bacterium
30 that includes wall-less cells as a natural stage in bacterial development.

31 INTRODUCTION

32 The cell wall, an essential component of virtually all bacteria, is a dynamic structure
33 that largely determines bacterial cell shape¹. It provides structural rigidity and
34 protection to osmotic stresses and forms the barrier between the bacterium and its
35 environment^{2,3}. Given its protective role, the cell wall and its biosynthetic enzymes
36 are targets of some of the best known antibiotics, including penicillin and
37 vancomycin^{4,5}. The synthesis of its major constituent, peptidoglycan (PG), involves
38 the activity of large protein complexes that cooperatively build and incorporate new
39 PG precursors into the growing glycan strands at the cell surface^{3,6,7}. These strands are
40 then cross-linked to form in essence a single, giant sacculus⁸. Major differences in
41 growth and cell division are seen between the planktonic firmicutes that grow via
42 lateral cell-wall growth, and the Actinobacteria, which include many multicellular
43 genera that form complex mycelia and grow via apical extension^{9,10}. A large number
44 of genes required for PG synthesis and cell division are organized in the highly
45 conserved *dcw* gene cluster (for division and cell wall synthesis), which contains the
46 cell division scaffold FtsZ^{11,12}. Some genes in this cluster have gained species-specific
47 functions, or have been lost during evolution. A well-known example is DivIVA: in
48 *Bacillus subtilis*, this protein is involved in septum-site localization by preventing
49 accumulation of the cell division initiator protein FtsZ¹³. In contrast, in filamentous
50 actinomycetes, DivIVA is a crucial component of the polarisome complex that drives
51 polar growth^{14,15}. As a consequence, *divIVA* is dispensable in *B. subtilis* but essential
52 in actinomycetes^{14,16}. Conversely, cell division is not essential for growth in
53 streptomycetes, and uniquely, *ftsZ* and various other genes that encode members of
54 the divisome can be deleted^{17,18}. These examples imply a major evolutionary
55 diversification that has separated Actinobacteria from other bacteria.

56 Although the cell wall is a vital structure for bacteria, several species can be
57 manipulated to produce cells that propagate without their wall, which are known as L-
58 forms¹⁹⁻²². Typically, this was done in an artificial way, by growing strains on osmo-
59 protective media in the presence of high levels of antibiotics targeting the enzymes
60 required for cell-wall synthesis²³⁻²⁵. More recently, L-form growth was also achieved
61 genetically by turning off PG synthesis^{20,26}. These approaches often yield unstable L-
62 form variants that quickly revert to the walled state when the inducing agents are
63 omitted. By contrast, stable L-forms can propagate indefinitely without the cell wall
64 and require two kinds of mutations²⁷. The first class of mutations leads to an increase
65 in membrane synthesis, either directly by increasing fatty acid biosynthesis, or
66 indirectly by reducing cell wall synthesis²⁸. The second class of mutations reduces
67 oxidative damage caused by reactive oxygen species, which are detrimental to
68 formation of L-forms²⁹. Notably, proliferation of L-forms is independent of the FtsZ-
69 based division machinery^{20,30}. Instead, their proliferation can be explained solely by
70 biophysical processes, in which an imbalance in the cell surface area to volume ratio
71 leads to spontaneous blebbing and the generation of progeny cells²⁸. This purely
72 biophysical mechanism of L-form proliferation is independent of the prokaryotic
73 lineage. This observation has led to the hypothesis that early life forms propagated in
74 a similar fashion well before the cell wall had evolved^{20,28,31}. Until now, no examples
75 are known of bacteria that generate L-form cells in the absence of the commonly used
76 inhibitors of cell-wall synthesis and that propagate without accumulating mutations.

77 Here we present evidence that filamentous actinomycetes have the natural
78 ability to form such wall-less cells. These cells can propagate in the wall-less state,
79 but can also revert to mycelial growth. Our work provides the first direct evidence
80 that L-form cells are a natural stage in bacterial life.

81 **Transitions between filamentous and L-form growth**

82 One of the key requirements for growth of L-form cells is the presence of an
83 osmotically balanced medium to prevent cell lysis. Unexpectedly, when the
84 actinomycete *Kitasatospora viridifaciens* (previously called *Streptomyces*
85 *viridifaciens*³²) is grown in liquid LPB (containing high levels of sucrose) in the
86 absence of any cell wall synthesis inhibitor, spherical vesicles were visible at low
87 frequency in the culture broth and in between the mycelial networks (Fig. 1A).
88 Replacing sucrose by an equimolar amount of NaCl also leads to the formation of
89 such vesicles, although they are less abundant and smaller than those formed in
90 LPMA containing sucrose (Extended Data Fig. S1B). In the absence of either
91 osmolyte, we could not detect any vesicles (Extended Data Fig. S1C). The spherical
92 vesicles often contained smaller vesicles inside and are surrounded by a membrane.
93 Importantly, staining with SYTO9 indicated that these vesicles contained DNA (Fig.
94 1B), while transmission EM indicated that they contained no cell wall (Fig. 1C, D),
95 which make them very reminiscent of L-form-like cells. Comparable DNA-containing
96 vesicles were also observed during growth of *Kitasatospora* strains MBT63 and
97 MBT66³², as well as *Streptomyces venezuelae*. However, they were not detected in
98 *Streptomyces coelicolor*, *Streptomyces griseus* or in *Streptomyces lividans* (Extended
99 Data Fig. S2).

100 To determine the location where these L-form-like cells originate from in the
101 context of the hyphae, we performed live imaging of growing colonies (Fig. 1E;
102 Extended Data Video S1). Approximately 7 hr after the visible emergence of germ
103 tubes, we detected a transient arrest in tip extension of the leading hypha (Fig. 1E,
104 $t=430$ mins). By that time, L-form-like cells became visible, which were extruded
105 from the hyphal tip (see arrow in Fig. 1E). After the extrusion process, the leading

106 hypha resumed elongation. Subapically, new branches became visible about 210
107 minutes after the first appearance of these cells (Extended Data Video S1, $t = 640$
108 min). Notably, such branches frequently also extruded L-form-like cells, similarly to
109 the leading hypha (Extended Data Video S2). This showed that the L-form-like cells
110 are produced at hyphal tips.

111 To study the viability of these L-form-like cells, we separated them from the
112 mycelia by filtration, and used the filtrate to inoculate fresh LPB medium. Strikingly,
113 these cells were able to proliferate in a manner reminiscent of the extrusion-resolution
114 mechanism that was previously described for proliferation of *B. subtilis* L-forms²⁰
115 (Fig. 1F; Extended Data Video S3). Apparently, these wall-less cells are natural L-
116 forms that can proliferate without the need for any genetic mutations. To discriminate
117 these natural L-forms from other stable and unstable L-forms generated by inducing
118 agents, we hereinafter refer to them as N-forms (for natural L-forms).

119 When N-forms were plated on solid LPMA medium, we noticed that some of
120 the cells generated colonies consisting of both mycelia and N-form cells, implying
121 that these N-forms can revert to mycelial growth (Fig. 1G; Extended Data Video S4).
122 To exclude that mycelial growth was caused by outgrowing spores present in the
123 filtrate, we also analysed a non-sporulating $\Delta ssgB$ mutant of *K. viridifaciens*
124 (Extended Data Fig. S3A-C). Like the wild-type strain, the N-forms of the $\Delta ssgB$
125 mutant propagated in the wall-less state in liquid, and reverted to mycelial growth on
126 solid medium (Extended Data Fig. S3D, E; Extended Data Video S5).

127 Altogether, this work thus presents the first example of a bacterium with the
128 natural ability to generate wall-less cells as a natural stage in bacterial life. These cells
129 can propagate without their cell wall, but can also revert to mycelial growth (Fig. 1H).

130

131 **Generation of the stable L-form lineage *alpha***

132 Although N-forms could propagate in the wall-less state, their phenotype was
133 reversible leading to mixtures of both hyphae and N-forms. To understand the
134 mechanism of this reversible metamorphosis, we aimed to generate a strain that could
135 reproducibly switch between an all-walled and completely wall-less state. To this end,
136 we exposed the wild-type strain to penicillin and lysozyme following a weekly sub-
137 culturing regime to obtain a derivative strain, which we designated *alpha*. As
138 intended, in sucrose-based media *alpha* exclusively proliferated in the L-form-like
139 state and showed no signs of reversion (Fig. 2A; Extended Data Video S6).
140 Characterization using transmission electron microscopy (TEM) confirmed that *alpha*
141 contained no PG-based cell wall (Fig. 2B). Excitingly, while *alpha* cells preferred the
142 L-form state, they still possessed the capacity of reversible metamorphosis. When
143 *alpha* was streaked onto plates lacking osmotic protectants, mycelial colonies were
144 obtained (Fig. 2C). Conversely, when mycelial colonies were transferred to plates
145 containing sucrose, the formation of L-form cells was readily induced, which, like in
146 the parental wild-type strain, emerged from the hyphal tip (Extended Data Video S7).
147 However, unlike the N-forms generated by the wild-type strain, the L-forms formed
148 by *alpha* indefinitely propagated in the wall-less state and did not revert to mycelial
149 growth on osmo-protective media.

150 To see if we could identify the mutations that predisposed proliferation in the
151 L-form state, we performed SNP analysis by comparing the genome sequence of
152 *alpha* to that of the parent DMS40239³³. This revealed that *alpha* had lost the 1.7MB
153 linear plasmid KVP1 that is present in the wild-type strain. In addition, three SNPs
154 were identified in the genome (Extended Data Table 1). One of the mutations mapped
155 to a non-coding DNA region between two genes encoding a putative glutamine-

156 fructose-6-phosphate transaminase and an ABC transporter, respectively. A second
157 mutation was identified in one of the two *lysX* genes (BOQ63_22710), and which
158 encodes a bifunctional phosphatidylglycerol lysyltransferase^{34,35}. This protein is
159 involved in lipid modification by transferring L-lysine from lysyl-tRNA to
160 phosphatidylglycerol. This mutation resulted in a T183I mutation in LysX. The third
161 SNP was in *uppP* (BOQ63_21575), resulting in an L58M change in its gene product
162 undecaprenyl-diphosphate phosphatase. This phosphatase is involved in the recycling
163 pathway of the carrier lipid undecaprenyl phosphate, which transports glycan
164 biosynthetic intermediates for cell wall synthesis³⁶. While their function related to
165 cell-wall or membrane synthesis is suggestive at least, and they may therefore
166 facilitate proliferation in the L-form state, none of them blocked reversible
167 metamorphosis.

168

169 **DivIVA is essential for reversible metamorphosis**

170 DivIVA is required for polar growth in *Streptomyces* and *Corynebacteria*^{14,16}. We
171 therefore wondered if DivIVA has a role in the formation or proliferation of *K.*
172 *viridifaciens* L-forms, which lack any obvious polarity. To address this question, we
173 first created plasmid pKR3, which leads to the constitutive expression of a C-terminal
174 eGFP fusion to DivIVA, which was partially active (see below). Analysis of a
175 transformant constitutively expressing DivIVA-eGFP revealed that the chimeric
176 protein localized to hyphal tips (Fig. 2D). This apical localization pattern is consistent
177 with earlier findings in streptomycetes¹⁴. Notably, some hyphae expressing the fusion
178 protein were wider and showed hyphal tip-splitting, which may be due to a polar
179 effect or deregulated expression of DivIVA. To localize DivIVA in the L-form state,
180 we made use of the fact that the generated strain reverts to the L-form mode-of-

181 growth on osmoprotective media. Despite the absence of polarity, L-forms containing
182 pKR3 typically showed one or two DivIVA foci per cell, which invariably were
183 localized to the membrane (Fig. 2D). In contrast, no foci were detected in L-form
184 cells constitutively expressing eGFP (pGreen) or those containing the empty plasmid
185 (pKR1).

186 We then constructed plasmids pKR4 to delete *divIVA* and pKR5 to delete a
187 large part of the *dcw* gene cluster, which includes *divIVA*¹¹ (Fig. 3A). Introduction of
188 these plasmids into *alpha* by transformation and subsequent screening yielded the
189 desired *divIVA* and *dcw* mutants. Western blot analysis using antibodies against
190 DivIVA of *Corynebacterium glutamicum* confirmed the absence of DivIVA in both
191 the *divIVA* and the *dcw* mutant (Fig. 3B). Analysis of growth in LPB medium or on
192 solid LPMA plates indicated that the L-form cells proliferated normally in the absence
193 of *divIVA* or part of the *dcw* gene cluster (Fig. 3C, D). However, when L-form cells
194 were plated on MYM medium, only the *alpha* strain could grow due to its ability to
195 form mycelial cells, while the *divIVA* and *dcw* mutants could not grow due to their
196 failure to undergo reversible metamorphosis (Fig. 3D). Introduction of plasmid pKR6
197 containing *sepF-sepG-divIVA* under control of their natural promoters restored growth
198 to the *divIVA* null mutant on MYM medium (Fig. 3D). To exclude that this was
199 caused by the additional *sepF* and *sepG* genes, we also introduced plasmid pKR7,
200 which expresses *divIVA* from the constitutive *gapI* promoter. This plasmid also
201 complemented growth of the *divIVA* mutant on MYM medium, thus establishing that
202 *divIVA* alone was sufficient to complement the *divIVA* null mutant (Fig. 3D).
203 Importantly, the DivIVA-eGFP fusion protein also restored filamentous growth to the
204 *divIVA* mutant, implying that the chimeric protein is largely functional *in vivo*.
205 However, some hyphae showed apical branching or tip-splitting indicative of polar

206 effects on growth and development (Extended Data Fig. S4). Altogether, these results
207 identify DivIVA as a key protein that is essential for reversible metamorphosis.

208

209 **Functional complementation of the *K. viridifaciens* *dcw* mutant by the**
210 ***S. coelicolor* *dcw* gene cluster**

211 The unique capacity of *alpha* to switch back-and-forth between a walled, filamentous
212 mode-of-growth and a wall-less L-form state provides a unique platform to apply an
213 engineering approach to cell morphology design. As a first step towards that goal, we
214 introduced the *dcw* gene cluster from *S. coelicolor* into the *K. viridifaciens* *dcw*
215 mutant (Fig. 3D, E). Excitingly, introduction of this gene cluster restored filamentous
216 growth and reversible metamorphosis (Fig. 3D, E), demonstrating that the *S.*
217 *coelicolor* *dcw* cluster functionally replaces the *dcw* cluster of *K. viridifaciens*. This is
218 an important observation as it also shows that the ability of *K. viridifaciens* to undergo
219 reversible metamorphosis is not dictated by specific adaptation in this organism of
220 genes within its *dcw* cluster. Staining of nascent PG synthesis by fluorescent
221 vancomycin (Van-FL) revealed a ladder-like staining pattern in the complemented
222 *dcw* mutant, which could not be discriminated from that observed for the *alpha* strain
223 growing as a mycelium (Fig. 3E). These ladders represent sites where PG-based septa
224 are formed in an FtsZ-dependent manner³⁷. Altogether, this demonstrates that the
225 mycelium formed by this ‘hybrid’ bacterium is established by the activity of the
226 macromolecular machinery of two different bacteria belonging to separate genera.
227 This paves the way for extending this principle with *dcw* gene clusters of
228 morphologically distinct bacteria, such as the unicellular actinobacteria
229 *Corynebacterium glutamicum* and *Mycobacterium tuberculosis*.

230

231 **DISCUSSION**

232 Filamentous actinomycetes have been studied for more than 50 years as a model for
233 multicellular bacterial development. We here provide compelling evidence that the
234 formation of wall-less cells is a natural, and previously unnoticed developmental stage
235 in these organisms. These natural wall-less cells, which we have dubbed N-forms, are
236 extruded from the hyphal tips, contain DNA and are viable as concluded from their
237 ability to form colonies. This work thus presents the first example of a bacterium with
238 the natural ability to generate wall-less cells and provides a major step in our ability to
239 reveal the ecological relevance of these enigmatic wall-less cells. It will be of key
240 interest to dissect how this unique morphogenetic switch is regulated and to disclose
241 how widespread this phenomenon is.

242 The spontaneous release of N-forms provides an important step forward
243 towards characterising where such cells are found in nature. Actinomycetes are
244 abundantly present in soil and marine environments and are known to interact with
245 many eukaryotic organisms, such as insects and plants^{38,39}. Interestingly, the phloem
246 of plants is rich in sucrose and provides a supportive environment to sustain wall-less
247 cells^{40,41}. Given their presence in soil environments, we envision that these
248 actinomycetes may associate with plant roots in their filamentous state, followed by a
249 switch to the wall-less state allowing them to quickly travel throughout the plant
250 tissue or via the phloem. In this way, they may be able to traverse long distances to
251 the sites where their activity is required, for instance in providing protection to the
252 plant mediated by their large repertoire of secondary metabolites they produce^{38,42}.
253 However, for other species this transient mode-of-growth, during which the wall-less
254 cells may escape from the plant immune system, could also help to cause damage to
255 plants. In this context it is interesting to note that we have been able to induce L-form

256 growth in the potato pathogen *Streptomyces scabies*, which, as a non-sporulating
257 strain, is known to traverse long distances within the plant (R. Loria, personal
258 communication). More generally, we suppose that wall-less cells may be more
259 commonly present in nature, but have simply been overlooked due to their specific
260 requirements for growth.

261 N-forms are released from hyphal tips, which contain extended membrane
262 structures³⁷. One of the key requirements for L-form proliferation is an upregulation
263 of membrane synthesis²⁸. We think that the presence of these extended membranes at
264 the hyphal tip may facilitate the formation of N-forms in these actinomycetes. Their
265 release from the hyphal tip coincides with an arrest in tip extension, indicating that
266 PG synthesis at those sites is transiently blocked. Notably, sequencing of the genome
267 of the stable L-form lineage *alpha* identified two mutations that may exert their effect
268 on PG synthesis. One mutation was identified in the non-coding region of a gene
269 encoding a protein controlling the flux of glucose in the hexosamine pathway,
270 ultimately leading to synthesis of PG precursors. A second mutation was found in
271 *uppP*, which is involved in PG precursor recycling. While these mutations may
272 regulate cell-wall precursor accumulation, none of them was essential for mycelial
273 growth. This can be derived from the fact that both N-forms as well as the L-forms
274 formed by *alpha* may revert to mycelial growth. However, the fact that the mutations
275 do not prevent mycelial growth does not rule out that they may have been essential for
276 the formation of a previous lineage that finally evolved into *alpha*. The role of the
277 mutations and their contribution to the formation of N-forms and proliferation of
278 *alpha* is under current investigation.

279 Summarising, our work on reversible metamorphosis provides the first
280 evidence for the existence of natural wall-less cells, and thereby broadens the large

281 diversity in bacterial cell shapes¹. Finally, it will enable us to design ‘hybrid’ bacteria
282 with dramatically changed cell morphologies by replacing some of the most
283 fundamental shape-defining genes. Ultimately, this should allow us to convert a truly
284 multicellular bacterium into a walled, unicellular derivative, which is not only
285 exciting from an evolutionary point-of-view, but which may also prove valuable as an
286 industrial workhorse for the biosynthesis of natural products. The functional
287 replacement of the *dcw* gene cluster between bacteria from distinct genera provides an
288 important first step towards that goal.

289

290 **METHODS**

291 **Strains and media**

292 Bacterial strains used in this study are shown in Extended Data Table 2. To obtain
293 sporulating cultures, *Streptomyces* and *Kitasatospora* species were grown at 30°C for
294 4 days on MYM medium, containing (w/v) 0.4% maltose, 0.4% yeast extract, 1%
295 malt extract, 2% Iberian agar, 0.2 (v/v) R5 trace elements⁴³. To support growth of
296 wall-less cells, strains were grown in liquid L-Phase Broth (LPB), containing (w/v)
297 0.15% yeast extract, 0.25% bacto-peptone, 0.15% oxoid malt extract, 0.5% glucose,
298 22% sucrose, 1.5% oxoid tryptone soya broth powder and 25 mM MgCl₂.

299 Alternatively, wall-less cells were propagated in liquid L-Phase Medium (LPM),
300 containing (w/v) 0.5% glucose, 0.5% yeast extract, 0.5% peptone, 20% sucrose,
301 0.01% MgSO₄·7H₂O, and 25 mM MgCl₂. Cultures were inoculated with 10⁶ spores
302 ml⁻¹ and grown in 250 ml flasks. Cultures were incubated at 30°C, while shaking at
303 100 rpm. For propagation of wall-less cells on solid medium, we used LPMA (i.e.
304 LPM supplemented with (w/v) 0.75% Iberian agar and 5% (v/v) horse serum).

305 Generation of the stable *K. viridifaciens* L-form lineage *alpha* was performed
306 in LPB, following the cultivation regime previously described⁴⁴. 50 ml cultures were
307 grown in 250 ml flasks in an orbital shaker at 100 rpm.

308 For general cloning purposes, *E. coli* strains DH5 α and JM109 were used,
309 while *E. coli* ET12567 and SCS110 were used to obtain unmethylated DNA
310 (Extended Data Table 2). *E. coli* strains were grown at 37 °C in LB medium,
311 supplemented with chloramphenicol (25 $\mu\text{g ml}^{-1}$), ampicillin (100 $\mu\text{g ml}^{-1}$), apramycin
312 (50 $\mu\text{g ml}^{-1}$), kanamycin (50 $\mu\text{g ml}^{-1}$), or viomycin (30 $\mu\text{g ml}^{-1}$), where necessary.

313

314 **Construction of plasmids**

315 All plasmids and primers used in this work are shown in Extended Data Table 3 and
316 Extended Data Table 4, respectively.

317

318 *Construction of the DivIVA localization construct pKR3*

319 To localize DivIVA, we first created plasmid pKR2 containing a viomycin resistance
320 cassette cloned into the unique NheI site of pIJ8630⁴⁵. To this end, the viomycin
321 resistance cassette was amplified from pIJ780⁴⁶ with the primers *vph*-FW-NheI and
322 *vph*-RV-NheI. Next, we amplified the strong constitutive *gapI* promoter as a 450 bp
323 fragment from the genome of *S. coelicolor* with the primers P_{GapI}-FW-BglII and
324 P_{GapI}-RV-XbaI. We also amplified the *divIVA* coding sequence (the +1 to +1335
325 region relative to the start codon of *divIVA* (BOQ63_31065) from the chromosome of
326 *K. viridifaciens* using primers *divIVA*-FW-XbaI and *divIVA*-no stop-RV-NdeI.
327 Finally, the promoter and *divIVA* coding sequence were cloned into pKR2 as a
328 BglII/XbaI and XbaI/NdeI fragment respectively, yielding plasmid pKR3.

329

330 *Construction of the deletion constructs pKR1, pKR4 and pKR5*

331 The *ssgB* mutant was created in *K. viridifaciens* using pKR1, which is a derivative of
332 the unstable plasmid pWHM3⁴⁷. In the *ssgB* mutant, nucleotides +20 to +261 relative
333 to the start codon of *ssgB* were replaced with the *loxP-apra* resistance cassette as
334 described⁴⁸. A similar strategy was used for the deletion of the *divIVA* gene or part of
335 the *dcw* cluster, using plasmids pKR4 and pKR5, respectively. In the *divIVA* deletion
336 mutant, nucleotides +205 to +349 relative to the start codon of *divIVA*
337 (BOQ63_31065) were replaced with the apramycin resistance cassette, whereas in the
338 *dcw* mutant the chromosomal region from +487 bp relative to the start of the *ftsW*
339 gene (BOQ63_31025) until +349 relative to the start of the *divIVA* gene was replaced
340 with the apramycin resistance marker.

341

342 *Construction of the complementation constructs pKR6 and pKR7*

343 The constructs pKR6 and pKR7 were created to complement the *divIVA* mutant. For
344 complementation of *divIVA* under control of its native promoter, the genomic
345 sequence from -1565 to +1357 relative to the translational start site of *divIVA* was
346 amplified from the chromosomal DNA of *K. viridifaciens* using the primers *sepF*-
347 *sepG-divIVA*-FW-BglII and *sepF-sepG-divIVA*-RV-XbaI. This product contained the
348 coding sequences of *sepF*, *sepG* and *divIVA* including the native *divIVA* promoter,
349 and was cloned into the integrative vector pIJ8600⁴⁵.

350 The pKR7 plasmid was constructed for the expression of *divIVA* from the
351 constitutive *gapI* promoter. To this end, the promoter region of *gapI* was amplified
352 with the primers P_{*gapI*}-FW-BglII and P_{*gapI*}-RV-XbaI using *S. coelicolor* genomic
353 DNA as the template. The *divIVA* coding sequence was amplified from the genome of
354 *K. viridifaciens* with the primers *divIVA*-XbaI-FW and *divIVA*-NdeI-RV. Finally, both

355 the *gapI* promoter and *divIVA* coding sequence were cloned as BglII/XbaI and
356 XbaI/NdeI fragments into the integrative vector pIJ8600⁴⁵. All constructs were
357 sequenced for verification.

358 For the orthologous complementation of the *K. viridifaciens dcw* mutant, the
359 *S. coelicolor* cluster from cosmid ST4A10⁴⁹ was used. The ST4A10 cosmid was cut
360 with BglII and ScaI, followed by gel extraction of a 13,268 bp BglII fragment,
361 encompassing the partial *S. coelicolor dcw* cluster. This fragment was subsequently
362 ligated into BglII-digested pIJ8600, yielding pKR8.

363

364 **Filtration of N-forms**

365 An individual colony of *K. viridifaciens* DSM40239 that had been grown on MYM
366 medium for 4 days was used to inoculate 50 ml LPB medium. The culture was grown
367 for 7 days at 30°C in an orbital shaker at 100 rpm. To separate the mycelium from the
368 N-forms, the culture was passed through a sterile filter made from an EcoCloth™
369 wiper. A subsequent filtration step was done by passing the N-forms through a 5 µm
370 Isopore™ membrane filter. The filtered cells were centrifuged at 1,000 rpm for 40
371 min, after which the supernatant was carefully removed by decantation to avoid
372 disturbance of the cells.

373

374 **Transformation of L-forms**

375 Transformation of *alpha* essentially followed the protocol for the rapid small-scale
376 transformation of *Streptomyces* protoplasts⁵⁰, with the difference that 50 µl cells from
377 a mid-exponential growing L-form culture were used instead of protoplasts.
378 Typically, 1 µg DNA was used for each transformation. Transformants were selected
379 by applying an overlay containing the required antibiotics in P-buffer after 20 hours.

380 Further selection of transformants was done on LPMA medium containing the
381 appropriate antibiotics.

382

383 **Microscopy**

384 Strains grown in LPB or LPMA were imaged using a Zeiss Axio Lab A1 upright
385 microscope equipped with an Axiocam Mrc. A thin layer of LPMA (without horse
386 serum) was applied to the glass slides to immobilize the cells prior to the microscopic
387 analysis.

388

389 *Fluorescence microscopy*

390 Fluorescence microscopy pictures were obtained with a Zeiss Axioscope A1 upright
391 fluorescence microscope with an Axiocam Mrc5 camera. Live cells were stained with
392 SYTO 9 (0.05 mM) and BODIPY vancomycin ($1 \mu\text{g ml}^{-1}$) for 10 min to detect DNA
393 and nascent PG, respectively. Stains were obtained from Molecular ProbesTM. The
394 fluorescent images were obtained using a 470/40 nm band pass excitation and a
395 505/560 band pass detection, using an 100x N.A. 1.3 objective. Stained live cells
396 where immobilized on microscope slides using a thin layer of LPMA (without horse
397 serum). To obtain a sufficiently dark background, the background of the images was
398 set to black. These corrections were made using Adobe Photoshop CS5.

399

400 *Time-lapse microscopy*

401 For visualization of N-form formation, spores of *K. viridifaciens* were pre-germinated
402 in TSBS (i.e. TSB containing 10% sucrose) for 5 hours. Aliquots of 10 μl of the
403 recovered germlings were placed in an ibiTreat 35 mm low imaging dish (ibidi®),
404 after which an LPMA patch was placed on top of the germlings. For visualization of

405 N-form growth, 50 μ l aliquots of filtered N-forms were used. All samples were
406 imaged for ~15 hours using an inverted Zeiss Axio Observer Z1 microscope equipped
407 with a Temp Module S (PECON) stage-top set to 30°C. Z-stacks with a 1 μ m spacing
408 were taken every six minutes using a 40x water immersion objective. Average
409 intensity projections of the in-focus frames were used to compile the final movies.
410 Light intensity over time was equalised using the correct bleach plugin of ImageJ
411 (version 1.51f).

412 To visualize the proliferation of *alpha* or filtered N-forms, cells were collected
413 and resuspended in 300 μ l LPB (containing 4-22% sucrose) and placed in the wells of
414 a chambered 8-well μ -slide (ibidi®). Cells were imaged on a Nikon Eclipse Ti-E
415 inverted microscope equipped with a confocal spinning disk unit (CSU-X1) operated
416 at 10,000 rpm (Yokogawa), using a 40x Plan Fluor Lens (Nikon) and illuminated in
417 bright-field. Images were captured every 2 minutes for 10-15 hours by an Andor iXon
418 Ultra 897 High Speed EM-CCD camera (Andor Technology). Z-stacks were acquired
419 at 0.2-0.5 μ m intervals using a NI-DAQ controlled Piezo element. During imaging
420 wall-less cells were kept at 30 °C using INUG2E-TIZ stage top incubator (Tokai Hit).
421

422 *Electron microscopy*

423 For transmission electron microscopy, L-forms obtained from a 7-day-old liquid
424 culture of the *K. viridifaciens alpha* strain were trapped in agarose blocks prior to
425 fixation with 1.5% glutaraldehyde. In contrast, cultures of the wild-type strain forming
426 N-forms were immediately fixed for an hour with 1.5% glutaraldehyde before being
427 filtered (see above). Filtered N-forms were then washed twice with 1X PBS prior to
428 embedding in 2% low melting agarose. A post-fixation step with 1% OsO₄ was
429 performed on both L- and N-forms. Samples were embedded in Epon and sectioned

430 into 70 nm slices. Samples were stained using uranyl-acetate (2%) and lead-citrate
431 (0.4%) if necessary. Samples were imaged using a Jeol 1010 or a Fei 12 BioTwin
432 transmission electron microscope.

433

434 **Genome sequencing and SNP analysis**

435 For genomic DNA isolation, the stable L-form cell line *alpha* was grown in LPB
436 medium for 3 days. After harvesting of the cells by centrifugation, genomic DNA was
437 isolated as described⁵⁰. Whole-genome sequencing and SNP analyses were performed
438 by BaseClear (Leiden, The Netherlands), using the sequence of the parental strain as a
439 reference³³.

440

441 **DivIVA detection using Western analysis**

442 To detect DivIVA using Western analysis, biomass of L-form strains was harvested
443 after 7 days of growth in LPB medium (100 rpm), while biomass of mycelial strains
444 was obtained from TSBS medium (200 rpm) after 17 hours. Cell pellets were washed
445 twice with 10% PBS, after which they were resuspended in 50mM HEPES pH 7.4, 50
446 mM NaCl, 0.5% Triton X-100, 1 mM PFMS and P8465 protease inhibitor cocktail
447 (Sigma). The cells and mycelia were disrupted with a Bioruptor Plus Sonication
448 Device (Diagenode). Complete lysis was checked by microscope, after which the
449 soluble cell lysate was separated by centrifugation at 13,000 rpm for 10 min at 4°C.
450 The total protein concentration in the cell lysates was quantified by BCA assay
451 (Sigma-Aldrich). Equal amounts of total proteins were separated with SDS-PAGE
452 using 12,5% gels. Proteins were transferred to polyvinylidene difluoride (PVDF)
453 membranes (GE Healthcare) with the Mini Trans-Blot® Cell (Bio-Rad Laboratories)
454 according to the manufacturer's instructions. DivIVA was detected using a 1:5,000

455 dilution of polyclonal antibodies raised against *Corynebacterium glutamicum*
456 DivIVA, and kindly provided by Professor Bramkamp (Ludwig-Maximilian-
457 Universität München). The secondary antibody, anti-rabbit IgG conjugated to alkaline
458 phosphatase (Sigma), was visualized with the BCIP/NBT Color Development
459 Substrate (Promega).

460

461 REFERENCES

- 462 1 Kysela, D. T., Randich, A. M., Caccamo, P. D. & Brun, Y. V. Diversity takes
463 shape: understanding the mechanistic and adaptive basis of bacterial
464 morphology. *PLoS Biol* **14**, e1002565, doi:10.1371/journal.pbio.1002565
465 (2016).
- 466 2 Cabeen, M. T. & Jacobs-Wagner, C. Bacterial cell shape. *Nat Rev Microbiol*
467 **3**, 601-610, doi:10.1038/nrmicro1205 (2005).
- 468 3 Typas, A., Banzhaf, M., Gross, C. A. & Vollmer, W. From the regulation of
469 peptidoglycan synthesis to bacterial growth and morphology. *Nat Rev*
470 *Microbiol* **10**, 123-136, doi:10.1038/nrmicro2677 (2012).
- 471 4 Park, J. T. & Strominger, J. L. Mode of action of penicillin. *Science* **125**, 99-
472 101 (1957).
- 473 5 Cho, H., Uehara, T. & Bernhardt, T. G. Beta-lactam antibiotics induce a lethal
474 malfunctioning of the bacterial cell wall synthesis machinery. *Cell* **159**, 1300-
475 1311, doi:10.1016/j.cell.2014.11.017 (2014).
- 476 6 Meeske, A. J. *et al.* SEDS proteins are a widespread family of bacterial cell
477 wall polymerases. *Nature* **537**, 634-638, doi:10.1038/nature19331 (2016).
- 478 7 Szwedziak, P. & Löwe, J. Do the divisome and elongasome share a common
479 evolutionary past? *Curr Opin Microbiol* **16**, 745-751,
480 doi:10.1016/j.mib.2013.09.003 (2013).
- 481 8 Höltje, J. V. Growth of the stress-bearing and shape-maintaining murein
482 sacculus of *Escherichia coli*. *Microbiol Mol Biol Rev* **62**, 181-203 (1998).
- 483 9 Claessen, D., Rozen, D. E., Kuipers, O. P., Sogaard-Andersen, L. & van
484 Wezel, G. P. Bacterial solutions to multicellularity: a tale of biofilms,
485 filaments and fruiting bodies. *Nat Rev Microbiol* **12**, 115-124,
486 doi:10.1038/nrmicro3178 (2014).
- 487 10 Flärdh, K. & Buttner, M. J. *Streptomyces* morphogenetics: dissecting
488 differentiation in a filamentous bacterium. *Nat Rev Microbiol* **7**, 36-49 (2009).
- 489 11 Vicente, M. & Errington, J. Structure, function and controls in microbial
490 division. *Mol Microbiol* **20**, 1-7 (1996).
- 491 12 Tamames, J., González-Moreno, M., Mingorance, J., Valencia, A. & Vicente,
492 M. Bringing gene order into bacterial shape. *Trends Genet* **17**, 124-126
493 (2001).
- 494 13 Marston, A. L., Thomaidis, H. B., Edwards, D. H., Sharpe, M. E. & Errington,
495 J. Polar localization of the MinD protein of *Bacillus subtilis* and its role in
496 selection of the mid-cell division site. *Genes Dev* **12**, 3419-3430 (1998).

- 497 14 Flårdh, K. Essential role of DivIVA in polar growth and morphogenesis in
498 *Streptomyces coelicolor* A3(2). *Mol Microbiol* **49**, 1523-1536 (2003).
- 499 15 Holmes, N. A. *et al.* Coiled-coil protein Scy is a key component of a
500 multiprotein assembly controlling polarized growth in *Streptomyces*. *Proc*
501 *Natl Acad Sci U S A* **110**, E397-406, doi:10.1073/pnas.1210657110 (2013).
- 502 16 Letek, M. *et al.* DivIVA is required for polar growth in the MreB-lacking rod-
503 shaped actinomycete *Corynebacterium glutamicum*. *J Bacteriol* **190**, 3283-
504 3292, doi:10.1128/JB.01934-07 (2008).
- 505 17 McCormick, J. R. Cell division is dispensable but not irrelevant in
506 *Streptomyces*. *Curr Opin Biotechnol* **12**, 689-698,
507 doi:10.1016/j.mib.2009.10.004 (2009).
- 508 18 McCormick, J. R., Su, E. P., Driks, A. & Losick, R. Growth and viability of
509 *Streptomyces coelicolor* mutant for the cell division gene *ftsZ*. *Mol Microbiol*
510 **14**, 243-254 (1994).
- 511 19 Klieneberger, E. The natural occurrence of pleuropneumonia-like organisms in
512 apparent symbiosis with *Streptobacillus moniliformis* and other bacteria. *J*
513 *Pathol Bacteriol* **40**, 93-105 (1935).
- 514 20 Leaver, M., Dominguez-Cuevas, P., Coxhead, J. M., Daniel, R. A. &
515 Errington, J. Life without a wall or division machine in *Bacillus subtilis*.
516 *Nature* **457**, 849-853, doi:10.1038/nature07742 (2009).
- 517 21 Frenkel, A. & Hirsch, W. Spontaneous development of L forms of
518 Streptococci requiring secretions of other bacteria or sulphhydryl compounds
519 for normal growth. *Nature* **191**, 728-730 (1961).
- 520 22 Studer, P. *et al.* Proliferation of *Listeria monocytogenes* L-form cells by
521 formation of internal and external vesicles. *Nat Commun* **7**, 13631,
522 doi:10.1038/ncomms13631 (2016).
- 523 23 Dienes, L. The Isolation of L type cultures from *Bacteroides* with the aid of
524 penicillin and their reversion into the usual bacilli. *J Bacteriol* **56**, 445-456
525 (1948).
- 526 24 Burmeister, H. R. & Hesseltine, C. W. Induction and propagation of a *Bacillus*
527 *subtilis* L form in natural and synthetic media. *J Bacteriol* **95**, 1857-1861
528 (1968).
- 529 25 Dell'Era, S. *et al.* *Listeria monocytogenes* L-forms respond to cell wall
530 deficiency by modifying gene expression and the mode of division. *Mol*
531 *Microbiol* **73**, 306-322, doi:10.1111/j.1365-2958.2009.06774.x (2009).
- 532 26 Domínguez-Cuevas, P., Mercier, R., Leaver, M., Kawai, Y. & Errington, J.
533 The rod to L-form transition of *Bacillus subtilis* is limited by a requirement for
534 the protoplast to escape from the cell wall sacculus. *Mol Microbiol* **83**, 52-66,
535 doi:10.1111/j.1365-2958.2011.07920.x (2012).
- 536 27 Errington, J., Mickiewicz, K., Kawai, Y. & Wu, L. J. L-form bacteria, chronic
537 diseases and the origins of life. *Philosophical Transactions of the Royal*
538 *Society B: Biological Sciences* **371**, doi:10.1098/rstb.2015.0494 (2016).
- 539 28 Mercier, R., Kawai, Y. & Errington, J. Excess membrane synthesis drives a
540 primitive mode of cell proliferation. *Cell* **152**, 997-1007,
541 doi:10.1016/j.cell.2013.01.043 (2013).
- 542 29 Kawai, Y. *et al.* Cell growth of wall-free L-form bacteria is limited by
543 oxidative damage. *Curr Biol* **25**, 1613-1618, doi:10.1016/j.cub.2015.04.031
544 (2015).

- 545 30 Mercier, R., Kawai, Y. & Errington, J. General principles for the formation
546 and proliferation of a wall-free (L-form) state in bacteria. *Elife* **3**,
547 doi:10.7554/eLife.04629 (2014).
- 548 31 Errington, J. L-form bacteria, cell walls and the origins of life. *Open Biol* **3**,
549 120143, doi:10.1098/rsob.120143 (2013).
- 550 32 Girard, G. *et al.* Analysis of novel kitasatosporae reveals significant
551 evolutionary changes in conserved developmental genes between
552 *Kitasatospora* and *Streptomyces*. *Antonie Van Leeuwenhoek* **106**, 365-380,
553 doi:10.1007/s10482-014-0209-1 (2014).
- 554 33 Ramijan, A. K., van Wezel, G. P. & Claessen, D. Genome sequence of the
555 filamentous actinomycete *Kitasatospora viridifaciens*. *Genome Announc*, In
556 press (2016).
- 557 34 Peschel, A. *et al.* *Staphylococcus aureus* resistance to human defensins and
558 evasion of neutrophil killing via the novel virulence factor MprF is based on
559 modification of membrane lipids with l-lysine. *J Exp Med* **193**, 1067-1076
560 (2001).
- 561 35 Maloney, E. *et al.* The two-domain LysX protein of *Mycobacterium*
562 *tuberculosis* is required for production of lysinylated phosphatidylglycerol and
563 resistance to cationic antimicrobial peptides. *PLoS Pathog* **5**, e1000534,
564 doi:10.1371/journal.ppat.1000534 (2009).
- 565 36 El Ghachi, M., Bouhss, A., Blanot, D. & Mengin-Lecreulx, D. The *bacA* gene
566 of *Escherichia coli* encodes an undecaprenyl pyrophosphate phosphatase
567 activity. *J Biol Chem* **279**, 30106-30113, doi:10.1074/jbc.M401701200
568 (2004).
- 569 37 Celler, K., Koning, R. I., Willemse, J., Koster, A. J. & van Wezel, G. P. Cross-
570 membranes orchestrate compartmentalization and morphogenesis in
571 *Streptomyces*. *Nat Commun* **7**, ncomms11836, doi:10.1038/ncomms11836
572 (2016).
- 573 38 Barka, E. A. *et al.* Taxonomy, physiology, and natural products of
574 *Actinobacteria*. *Microbiol Mol Biol Rev* **80**, 1-43, doi:10.1128/MMBR.00019-
575 15 (2016).
- 576 39 Seipke, R. F., Kaltenpoth, M. & Hutchings, M. I. *Streptomyces* as symbionts:
577 an emerging and widespread theme? *FEMS Microbiol Rev* **36**, 862-876,
578 doi:10.1111/j.1574-6976.2011.00313.x (2012).
- 579 40 Amijee, F., Allans, E. J., Waterhouse, R. N., Glover, L. A. & Paton, A. M.
580 Non-pathogenic association of L-form bacteria (*Pseudomonas syringae* pv.
581 *phaseolicola*) with bean plants (*Phaseolus vulgaris* L.) and its potential for
582 biocontrol of halo blight disease. *Biocontrol Sci Technol* **2**, 203-214 (1992).
- 583 41 Allan, E. J., Hoischen, C. & Gumpert, J. Bacterial L-forms. *Adv Appl*
584 *Microbiol* **68**, 1-39, doi:10.1016/S0065-2164(09)01201-5 (2009).
- 585 42 Viaene, T., Langendries, S., Beirinckx, S., Maes, M. & Goormachtig, S.
586 *Streptomyces* as a plant's best friend? *FEMS Microbiol Ecol* **92**,
587 doi:10.1093/femsec/fiw119 (2016).
- 588 43 Stuttard, C. Temperate phages of *Streptomyces venezuelae*: lysogeny and host
589 specificity shown by phages SV1 and SV2. *Journal of General Microbiology*
590 **128**, 115-121 (1982).
- 591 44 Innes, C. M. J. & Allan, E. J. Induction, growth and antibiotic production of
592 *Streptomyces viridifaciens* L-form bacteria. *J Appl Microbiol* **90**, 301-308
593 (2001).

- 594 45 Sun, J., Kelemen, G. H., Fernández-Abalos, J. M. & Bibb, M. J. Green
595 fluorescent protein as a reporter for spatial and temporal gene expression in
596 *Streptomyces coelicolor* A3(2). *Microbiology* **145**, 2221-2227 (1999).
- 597 46 Gust, B., Challis, G. L., Fowler, K., Kieser, T. & Chater, K. F. PCR-targeted
598 *Streptomyces* gene replacement identifies a protein domain needed for
599 biosynthesis of the sesquiterpene soil odor geosmin. *Proc Natl Acad Sci U S A*
600 **100**, 1541-1546, doi:10.1073/pnas.0337542100 (2003).
- 601 47 Vara, J., Lewandowska-Skarbek, M., Wang, Y. G., Donadio, S. & Hutchinson,
602 C. R. Cloning of genes governing the deoxysugar portion of the erythromycin
603 biosynthesis pathway in *Saccharopolyspora erythraea* (*Streptomyces*
604 *erythreus*). *J Bacteriol* **171**, 5872-5881 (1989).
- 605 48 Świątek, M. A., Tenconi, E., Rigali, S. & van Wezel, G. P. Functional analysis
606 of the N-acetylglucosamine metabolic genes of *Streptomyces coelicolor* and
607 role in control of development and antibiotic production. *J Bacteriol* **194**,
608 1136-1144, doi:10.1128/JB.06370-11 (2012).
- 609 49 Redenbach, M. *et al.* A set of ordered cosmids and a detailed genetic and
610 physical map for the 8 Mb *Streptomyces coelicolor* A3(2) chromosome. *Mol*
611 *Microbiol* **21**, 77-96 (1996).
- 612 50 Kieser, T., Bibb, M. J., Buttner, M. J., Chater, K. F. & Hopwood, D. A.
613 *Practical Streptomyces genetics*. (The John Innes Foundation, 2000).
- 614

615 **Acknowledgements**

616 We would like to thank Tim Janson for microscopy support and Marc Bramkamp for
617 providing us with antibodies. We are indebted to Mark Leaver, Roberto Kolter,
618 Danny Rozen, Ben Lugtenberg and Paul Hooykaas for critical reading of the
619 manuscript. This work was supported by a VIDI grant from the Dutch Applied
620 Research Council (STW 12957).

621

622 **Author Contributions**

623 K.R., J.W., E.U., A.J.W., A.M., A.B., D.H., G.P.W. and D.C. collected the data and
624 aided in data analysis. D.C. and G.P.W. designed the experiments and supervised the
625 research. K.R., G.P.W. and D.C. wrote the manuscript with input from all co-authors.

626

627 **Competing Financial Interests**

628 The authors declare there are no competing financial interests

629

630 **LEGENDS**

631 **Figure 1. Wall-less cells are a natural stage in bacterial development.**

632 (A) In media containing high levels of sucrose, the filamentous bacterium *K.*
633 *viridifaciens* forms spherical vesicles (arrowheads), which stain with the dye SYTO9
634 (B). Transmission electron micrographs indicate that these vesicles are cells that lack
635 the cell wall (C, D). The arrowheads indicate the cell membrane. (E) These wall-less
636 cells (arrows) are extruded from the hyphal tip. Arrowheads indicate new branches,
637 while “S” designates the spore. Images were taken from Extended Data Video S1. (F)
638 Phase-contrast images from Extended Data Video S3 showing proliferation of wall-
639 less cells in LPB medium. The times are indicated in HH:MM. The cell indicated with

640 an asterisk had entered the field after 38 mins. (G) Reversion of wall-less cells to
641 hyphal growth yields colonies consisting of hyphae and (newly-formed) wall-less
642 cells. Images were taken from Extended Data Video S4. (H) Model indicating that
643 wall-less cells (or N-forms) are a natural stage in bacterial development. On osmo-
644 protective media, vegetative hyphae generate N-form cells that either proliferate
645 transiently in the wall-less state, or immediately revert to mycelial growth (right).
646 Reversion to mycelial growth allows the strain to complete its canonical life cycle
647 (left). Scale bars represent 1 μm (D), 5 μm (C, F), 10 μm (A, B, E) or 20 μm (G).

648

649 **Figure 2. Characterization of the stable L-form cell line *alpha*.** (A) Phase-contrast
650 images from Extended Data Video S6, which demonstrate the proliferation of *alpha*
651 in the L-form state. The arrowhead points to the dividing mother cell. Please note that
652 after the generation of new progeny the mother cell lysis (indicated with an asterisk).
653 (B) Transmission electron micrograph showing an *alpha* cell lacking the cell wall. (C)
654 On plates containing sucrose and MgCl_2 , *alpha* forms colonies exclusively containing
655 L-forms, while it forms mycelial colonies on plates without these supplements. (D) L-
656 forms of *alpha* (*alpha*^L) transformed with pGreen, leading to the constitutive
657 expression of eGFP, show a diffuse cytosolic GFP signal. By contrast, L-form cells
658 containing pKR3, thereby expressing eGFP fused to DivIVA, show distinct foci
659 localized to the membrane. When the strains are grown as a mycelium (*alpha*^M),
660 DivIVA-eGFP localized to the hyphal tips (arrowheads). No fluorescence is observed
661 in cells or mycelium containing the control plasmid pKR1. Scale bars represent 500
662 nm (B), 5 μm (A), 10 μm (D) or 20 μm (C).

663

664 **Figure 3. Reversible metamorphosis depends on DivIVA.** (A) Illustration of the
665 *dcw* clusters in *alpha* and the derivative strains lacking *divIVA* or part of the *dcw*
666 cluster. (B) Western analysis confirming the absence of DivIVA in the $\Delta divIVA$ and
667 Δdcw mutants. Introduction of *divIVA* under control of its own (pKR6) or the *gapI*
668 (pKR7) promoter restores the presence of DivIVA. Likewise, introduction of the
669 *S. coelicolor dcw* gene cluster (on pKR8) in the $\Delta divIVA$ or Δdcw mutant strains
670 restores the presence of DivIVA. MW is the molecular weight in kDa. (C)
671 Comparable growth between *alpha* (solid black line) and the $\Delta divIVA$ (dashed line)
672 and the Δdcw mutants (dotted line) in liquid LPB medium. (D) The mutant strains
673 lacking *divIVA* can no longer grow on MYM plates lacking sucrose and $MgCl_2$. (D)
674 Reintroduction of the *S. coelicolor dcw* gene cluster (on pKR8) in the Δdcw mutant
675 restores mycelial growth, including septal PG synthesis, as revealed by staining with
676 fluorescent vancomycin (vanFL). Scale bar represents 5 μm .

677

678 **Extended Data Figure S1. Osmolytes are required for the formation of wall-less**
679 **cells.** The addition of 0.6M sucrose (A) or NaCl (B) to LPB medium is required for
680 the formation of wall-less cells. No wall-less cells are detected without the addition of
681 osmolytes (C). Scale bars represent 20 μm .

682

683 **Extended Data Figure S2. Formation of wall-less cells in *Streptomyces* and**
684 ***Kitasatospora* species.** Unlike *Streptomyces coelicolor* (A), *Streptomyces lividans* (B)
685 and *Streptomyces griseus* (C), wall-less (arrowheads) are evident in *Streptomyces*
686 *venezuelae* (D), and *Kitasatospora* strains MBT63 (E) and MBT66 (F) grown in LPB
687 medium. The inlays show magnified versions of wall-less cells in these species. (G-I).

688 Visualization of DNA in wall-less cells using SYTO9. Scale bars represent 5 μm
689 (inlays), 10 μm (G-I) or 20 μm (A-F).

690

691 **Extended Data Figure S3. Reversible metamorphosis in the *K. viridifaciens* ΔssgB**

692 **mutant.** (A) Deletion of *ssgB* in *K. viridifaciens* blocks the formation of grey spores.

693 (B, C) Transmission electron micrographs of N-forms of the ΔssgB mutant strain

694 indicates that they lack the cell wall. The arrowhead indicates the cell membrane (C).

695 (D) Phase-contrast images from Extended Data Video S5 showing N-form

696 proliferation in liquid medium. The times are indicated in HH:MM. (E) Plating of N-

697 forms of the *ssgB* mutant on LPMA yields colonies consisting of mycelia and N-

698 forms. Scale bars represent 200 nm (C), 2 μm (B), 10 μm (D) or 20 μm (E).

699

700 **Extended Data Figure S4. Functional complementation of the ΔdivIVA mutant**

701 **by DivIVA-eGFP** The DivIVA-eGFP fusion expressed from pKR3 restores

702 filamentous growth of the *divIVA* mutant, and localizes to the hyphal tips

703 (arrowheads). Scale bars represent 10 μm .

704

705 **Extended Data Video S1. Apical extrusion of N-forms in *K. viridifaciens*.** N-forms

706 are extruded from the hyphal tip after 430 min, coinciding with a transient arrest in tip

707 growth. After extrusion of the N-forms, the hypha resumes elongation after 540 min,

708 while subapically new branches become visible after 620 min. The times are indicated

709 in min.

710 **Extended Data Video S2. Extrusion of N-forms from branches in *K. viridifaciens*.**

711 N-forms are extruded from the tips of branches that are formed subapically.

712

713 **Extended Data Video S3. Proliferation of N-forms.** N-forms from *K. viridifaciens*
714 proliferate in the wall-less state in liquid LPB medium. The arrowhead indicates the
715 cells that are shown in Fig. 1F. The times are indicated in HH:MM. The scale bar
716 represents 10 μm .

717

718 **Extended Data Video S4. Proliferation and reversion of wild-type N-forms.**

719 Growth and reversion of N-forms on solid LPMA medium yields colonies consisting
720 of both hyphae and N-forms. The times are indicated in HH:MM. The scale bar
721 indicates 20 μm .

722

723 **Extended Data Video S5. Proliferation of N-forms of the ΔssgB mutant strain.** N-

724 forms of the ΔssgB mutant strain proliferate in the wall-less state in liquid LPB
725 medium. The arrowhead indicates the cell that is shown in Extended Data Fig. S3D.
726 The times are indicated in HH:MM. The scale bar represents 10 μm .

727

728 **Extended Data Video S6. Proliferation of *alpha* in the L-form state.** The stable
729 cell line *alpha* exclusively proliferates in the L-form state in medium containing high
730 levels of sucrose. The arrowhead indicates the proliferating cell that is used to make
731 Fig. 2A. The times are indicated in HH:MM. The scale bar represents 10 μm .

732

733 **Extended Data Video S7. L-forms are released from hyphal tips in *alpha*.**

734 Transfer of mycelial colonies of *alpha* on plates containing high levels of sucrose
735 leads to the extrusion of L-forms from the hyphal tips. The times are indicated in min.

Extended Data Table 1. Detected single nucleotide polymorphisms (SNPs) in the chromosome of *alpha*.

SNP	Position in genome	Locus	Variant in wild-type	Variant in <i>alpha</i>	Effect on protein	Protein function
1	546 832	NCR	C	A	None	Unknown
2	3 549 271	BOQ63_22710	G	A	LysX ^{T183I}	Biosynthesis of lysyl-phosphatidyl glycerol
3	3 297 354	BOQ63_21575	C	A	UppP ^{L58M}	Dephosphorylation of undecaprenyl pyrophosphate

NCR: non-coding region. LysX: phosphatidylglycerol lysyltransferase, UppP: undecaprenyl diphosphatase.

Extended Data Table 2. Strains used in this study.

Strains	Genotype	Reference
<i>Escherichia coli</i> strains		
DH5 α	F ⁻ Φ 80' <i>lacZ</i> Δ M15 Δ (<i>lacZYA-argF</i>)U169 <i>recA1 endA1 hsdR17</i> (rK ⁻ , mK ⁺) <i>phoA</i> <i>supE44 thi-1 gyrA96 relA1</i> λ	1
JM109	<i>recA1 endA1 gyrA96 thi hsdR17 supE44</i> <i>relA1</i> λ Δ (<i>lac-proAB</i>) [F' <i>traD36 proAB</i> <i>lacI</i> ^f Δ M15]	2
ET12567	F ⁻ <i>dam-13::Tn9</i> (Chl ^R) <i>dcm-6 hsdM hsdR</i> <i>recF143 zjj-201::Tn10 galK2 galT22</i> <i>ara14 lacY1 xyl-5 leuB6 thi-1 tonA31</i> <i>rpsL136 hisG4 tsx78 mtl-1 glnV44</i>	3
SCS110	<i>rpsL</i> (Str ^R) <i>thr leu endA thi-1 lacY galK</i> <i>galT ara tonA tsx dam dcm supE44</i> Δ (<i>lac-</i> <i>proAB</i>) [F' <i>traD36 proAB lacI</i> ^f Δ M15]	4
<i>Streptomyces</i> / <i>Kitasatospora</i> strains		
<i>Streptomyces coelicolor</i> A3(2) M145	Wild-type	Lab collection
<i>Streptomyces lividans</i> 1326	Wild-type	Lab collection
<i>Streptomyces griseus</i>	Wild-type	Lab collection
<i>Streptomyces venezuelae</i> DIVERSA	Wild-type	Lab collection
<i>Kitasatospora viridifaciens</i> DSM40239	Wild-type	Lab collection
<i>Kitasatospora</i> sp. MBT63	Wild-type	5
<i>Kitasatospora</i> sp. MBT66	Wild-type	5
<i>K. viridifaciens</i> Δ <i>ssgB</i>	<i>K. viridifaciens</i> DSM40239 derivative in which the <i>ssgB</i> gene has been replaced by an apramycin resistance marker	This work
<i>K. viridifaciens</i> L-form strains		
<i>alpha</i>	Stable <i>K. viridifaciens</i> L-form cell line	This work
Δ <i>divIVA</i>	<i>alpha</i> derivative in which the <i>divIVA</i> gene has been replaced by an apramycin resistance marker	This work
Δ <i>dcw</i>	<i>alpha</i> derivative in which part of the <i>dcw</i> gene cluster has been replaced by an apramycin resistance marker. The deleted genes include <i>ftsW</i> , <i>murG</i> , <i>ftsQ</i> , <i>ftsZ</i> , <i>ylmD</i> , <i>ylmE</i> , <i>sepG</i> , <i>sepF</i> , and <i>divIVA</i> .	This work

References

- 1 Hanahan, D. Studies on transformation of *Escherichia coli* with plasmids. *J Mol Biol* **166**, 557-580 (1983).
- 2 Yanisch-Perron, C., Vieira, J. & Messing, J. Improved M13 phage cloning vectors and host strains: nucleotide sequences of the M13mp18 and pUC19 vectors. *Gene* **33**, 103-119 (1985).
- 3 MacNeil, D. J. *et al.* Analysis of *Streptomyces avermitilis* genes required for avermectin biosynthesis utilizing a novel integration vector. *Gene* **111**, 61-68 (1992).
- 4 Jerpseth, B. & Kretz, B. L. SCS110: *dam*-, *dcm*-, *endA*- Epicurian coli® competent cells. *Strategies* **6**, 22 (1993).
- 5 Girard, G. *et al.* Analysis of novel kitasatosporae reveals significant evolutionary changes in conserved developmental genes between *Kitasatospora* and *Streptomyces*. *Antonie Van Leeuwenhoek* **106**, 365-380, doi:10.1007/s10482-014-0209-1 (2014).

Extended Data Table 3. Plasmids used in this study.

Plasmid	Description and relevant features	Reference
pWHM3	Unstable, multi-copy and self-replicating <i>Streptomyces</i> vector. Contains thiostrepton and ampicillin resistance cassette.	1
pIJ780	Plasmid containing a viomycin (<i>vph</i>) resistance cassette.	2
pIJ8600	<i>E. coli</i> – <i>Streptomyces</i> shuttle vector containing the ϕ C31 <i>attP-int</i> region for genomic integration. Confers resistance to apramycin and thiostrepton.	3
pIJ8630	<i>E. coli</i> – <i>Streptomyces</i> shuttle vector containing the ϕ C31 <i>attP-int</i> region for genomic integration. Confers resistance to apramycin	3
pGreen	pIJ8630 containing the <i>eGFP</i> gene under control of the constitutive <i>gap1</i> promoter of <i>S. coelicolor</i> .	4
ST4A10	Supercosmid fragment containing SCO2068-SCO2105 (43 147bp). Confers resistance to ampicillin and kanamycin.	5
pKR1	pWHM3 containing the flanking regions of the <i>K. viridifaciens ssgB</i> gene interspersed by the <i>apra-loxP</i> cassette.	This study
pKR2	pIJ8630 derivative containing the viomycin resistance cassette from pIJ780 cloned into the unique <i>NheI</i> site.	This work
pKR3	pKR2 derivative containing a C-terminal <i>eGFP</i> fusion to <i>divIVA</i> of <i>K. viridifaciens</i> under control of the <i>gap1</i> promoter of <i>S. coelicolor</i> .	This work
pKR4	pWHM3 containing the flanking regions of the <i>K. viridifaciens divIVA</i> gene interspersed by the <i>apra-loxP</i> cassette.	This work
pKR5	pWHM3 derivative containing the flanking regions around the <i>K. viridifaciens dcw</i> gene cluster interspersed by the <i>apra-loxP</i> cassette.	This work
pKR6	pIJ8600 containing <i>divIVA</i> of <i>K. viridifaciens</i> under control of its native promoter (which includes the coding sequences of <i>sepF</i> and <i>sepG</i>).	This work
pKR7	pIJ8600 containing the <i>divIVA</i> gene of <i>K. viridifaciens</i> under control of the <i>gap1</i> promoter of <i>S. coelicolor</i> .	This work
pKR8	pIJ8600 containing a 13,268 bp <i>BglII</i> fragment encompassing the <i>murD</i> , <i>ftsW</i> , <i>murG</i> , <i>ftsQ</i> , <i>ftsZ</i> , <i>ylmD</i> , <i>ylmE</i> , <i>sepF</i> , <i>sepG</i> and <i>divIVA</i> genes of the <i>S. coelicolor dcw</i> gene cluster.	This work

References

- 1 Vara, J., Lewandowska-Skarbek, M., Wang, Y. G., Donadio, S. & Hutchinson, C. R. Cloning of genes governing the deoxysugar portion of the erythromycin biosynthesis pathway in *Saccharopolyspora erythraea* (*Streptomyces erythreus*). *J Bacteriol* **171**, 5872-5881 (1989).
- 2 Gust, B., Challis, G. L., Fowler, K., Kieser, T. & Chater, K. F. PCR-targeted *Streptomyces* gene replacement identifies a protein domain needed for biosynthesis of the sesquiterpene soil odor geosmin. *Proc Natl Acad Sci U S A* **100**, 1541-1546, doi:10.1073/pnas.0337542100 (2003).
- 3 Sun, J., Kelemen, G. H., Fernández-Abalos, J. M. & Bibb, M. J. Green fluorescent protein as a reporter for spatial and temporal gene expression in *Streptomyces coelicolor* A3(2). *Microbiology* **145**, 2221-2227 (1999).
- 4 Zacchetti, B. *et al.* Aggregation of germlings is a major contributing factor towards mycelial heterogeneity of *Streptomyces*. *Sci Rep* **6**, 27045, doi:10.1038/srep27045 (2016).
- 5 Redenbach, M. *et al.* A set of ordered cosmids and a detailed genetic and physical map for the 8 Mb *Streptomyces coelicolor* A3(2) chromosome. *Mol Microbiol* **21**, 77-96 (1996).

Extended Data Table 4. Primers used in this study.

Restriction sites are underlined.

Primer	Sequence (5' – 3')
P1- <i>ssgB</i> -FW	GACGAATTCAGGCGTCAGAAACGGGTATC
P2- <i>ssgB</i> -RV	GAAGTTATCCATCACCTCTAGAGCTGACCGTGGTGTTCATAAGC
P3- <i>ssgB</i> -FW	GAAGTTATCGCGCATCTCTAGACTGAGCTCTCCGGAAGGAGAA
P4- <i>ssgB</i> -RV	GACAAGCTTTCTACCTGACCGGGCTGTT
Delcheck- <i>ssgB</i> -FW	GGCGGGTACTCCGTGATGATTC
Delcheck- <i>ssgB</i> -RV	AGCTTTCGGCGAGGATGTGG
<i>vph</i> -FW-NheI	GACGCTAGCGGCTGACGCCGTTGGATACACCAAG
<i>vph</i> -RV-NheI	GACGCTAGCAATCGACTGGCGAGCGGCATCCTAC
P _{Gap1} -FW-BglII	GATTACAGATCTCCGAGGGCTTCGAGACC
P _{Gap1} -RV-XbaI	GATGACTCTAGACCGATCTCCTCGTTGGTAC
<i>divIVA</i> -FW-XbaI	GTCAAGCTTCTAGAAATGCCATTGACCCCGAGGA
<i>divIVA</i> -Nostop-RV-NdeI	GACCATATGGTTGTGCGCCGTCCTCGTCAATCAGG
P1- <i>divIVA</i> -FW	GACGACGAATTCGTGTGATGACCGTCGCTCCACTG
P2- <i>divIVA</i> -RV	GACGACTCTAGACTTCCGCATGTTGGCCTGGTTC
P1- <i>dcw</i> -FW	GACGAATTCCTCCGCGAGGTCACGTACATC
P2- <i>dcw</i> -RV	GACTCTAGAAGAGCACCAGTGCGAGCTTG
P3- <i>dcw</i> -FW	GACTCTAGAAGCAGCAGATGGGCAACCAG
P4- <i>dcw</i> -RV	GATAAGCTTCCCGGCTACAACCTCAGTTGTC
Delcheck- <i>divIVA</i> -FW	TGACCCGGCCACGACTTTAC
Delcheck- <i>divIVA</i> -RV	GGACGCCCTCAACAAAC
Delcheck- <i>dcw</i> -FW	CCAGAACTGGCTGGATTTTCG
Delcheck- <i>dcw</i> -RV	GTCTCCAGGTACGACTTCAG
<i>ftsZ</i> -int-FW	ATGTGGGCCGCTGAACTCACC
<i>ftsZ</i> -int-RV	GACCGCACCGAAGATGATG
<i>ftsQ</i> -int-FW	CCTGGGTGGTGTCTTCTC
<i>ftsQ</i> -int-RV	CCTGGGTGGTGTCTTCTC
<i>sepF-sepG-divIVA</i> -FW-BglII	GACGACAGATCTTGTGATGACCGTCGCTCCACTG
<i>sepF-sepG-divIVA</i> -RV-XbaI	GACGACTCTAGAAACAAACCCGGCTACAACCTCAGTTGTC
<i>divIVA</i> -XbaI-FW	GTCAAGCTTCTAGAAATGCCATTGACCCCGAGGA
<i>divIVA</i> -NdeI-RV	GATCGAATTCATATGCCCGGCTACAACCTCAGTTGTC
<i>divIVA</i> seq1-FW	AGCAGCAGATGGGCAACCAG
<i>divIVA</i> seq2-FW	CGCGTCTGAAGTCGTACCTG
<i>divIVA</i> seq-RV	ACCTCGTCCTCGTCATAGC
SCO2079_F-520	TCACGGCGCTGTGCAAGGAGGCCG
SCO2079_R+1162	CTCATCGAGGAAGGCATCGACCTC
<i>divIVAsco</i> -FW	AAGGCTACGCCGTACTACAG
<i>divIVAsco</i> -RV	AGATACGGGCTTGCCGAATG

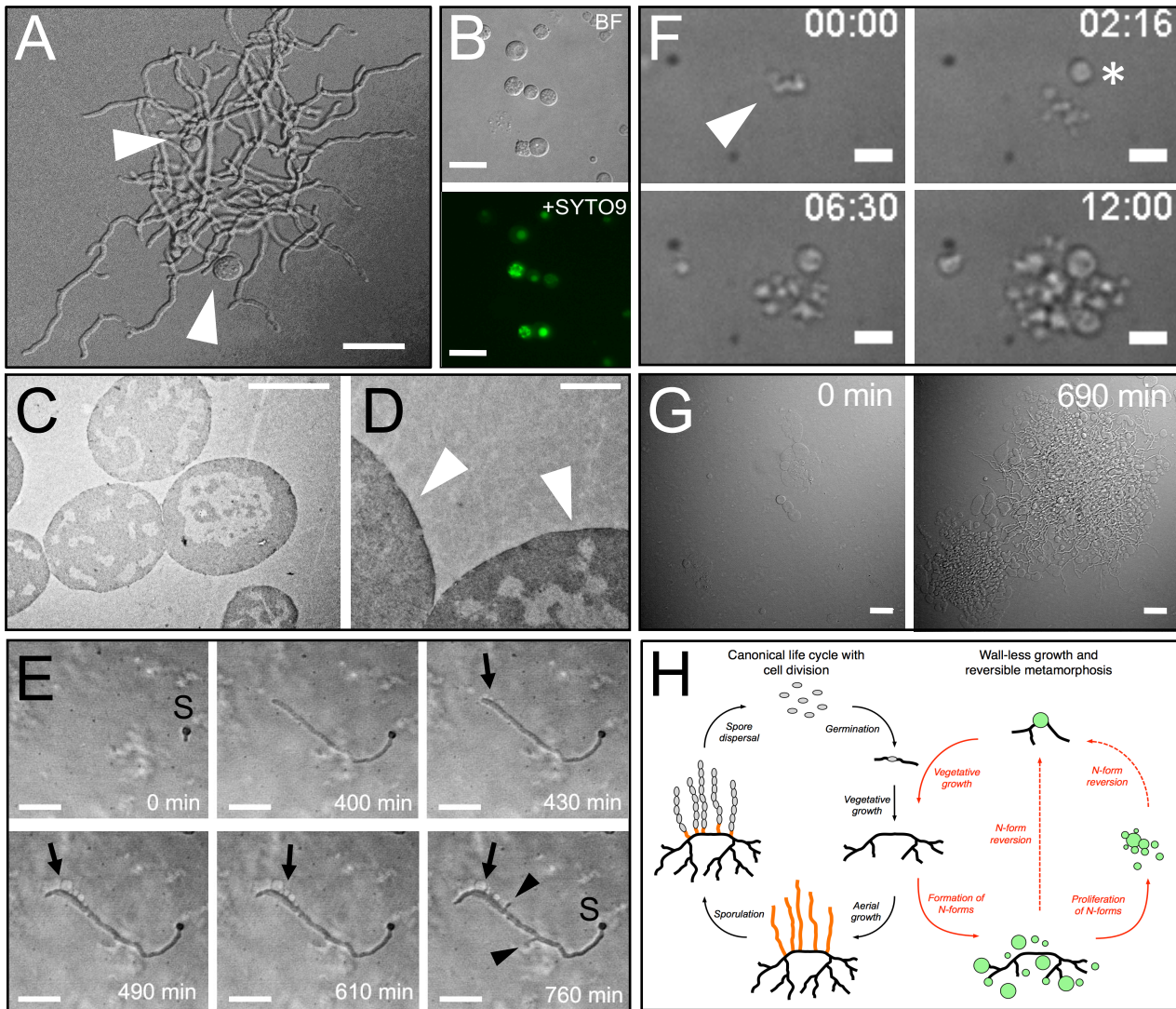


Figure 1. Wall-less cells are a natural stage in bacterial development.

(A) In media containing high levels of sucrose, the filamentous bacterium *K. viridifaciens* forms spherical vesicles (arrowheads), which stain with the dye SYTO9 (B). Transmission electron micrographs indicate that these vesicles are cells that lack the cell wall (C, D). The arrowheads indicate the cell membrane. (E) These wall-less cells (arrows) are extruded from the hyphal tip. Arrowheads indicate new branches, while “S” designates the spore. Images were taken from Extended Data Video S1. (F) Phase-contrast images from Extended Data Video S3 showing proliferation of wall-less cells in LPB medium. The times are indicated in HH:MM. The cell indicated with an asterisk had entered the field after 38 mins. (G) Reversion of wall-less cells to hyphal growth yields colonies consisting of hyphae and (newly-formed) wall-less cells. Images were taken from Extended Data Video S4. (H) Model indicating that wall-less cells (or N-forms) are a natural stage in bacterial development. On osmo-protective media, vegetative hyphae generate N-form cells that either proliferate transiently in the wall-less state, or immediately revert to mycelial growth (right). Reversion to mycelial growth allows the strain to complete its canonical life cycle (left). Scale bars represent 1 μm (D), 5 μm (C, F), 10 μm (A, B, E) or 20 μm (G).

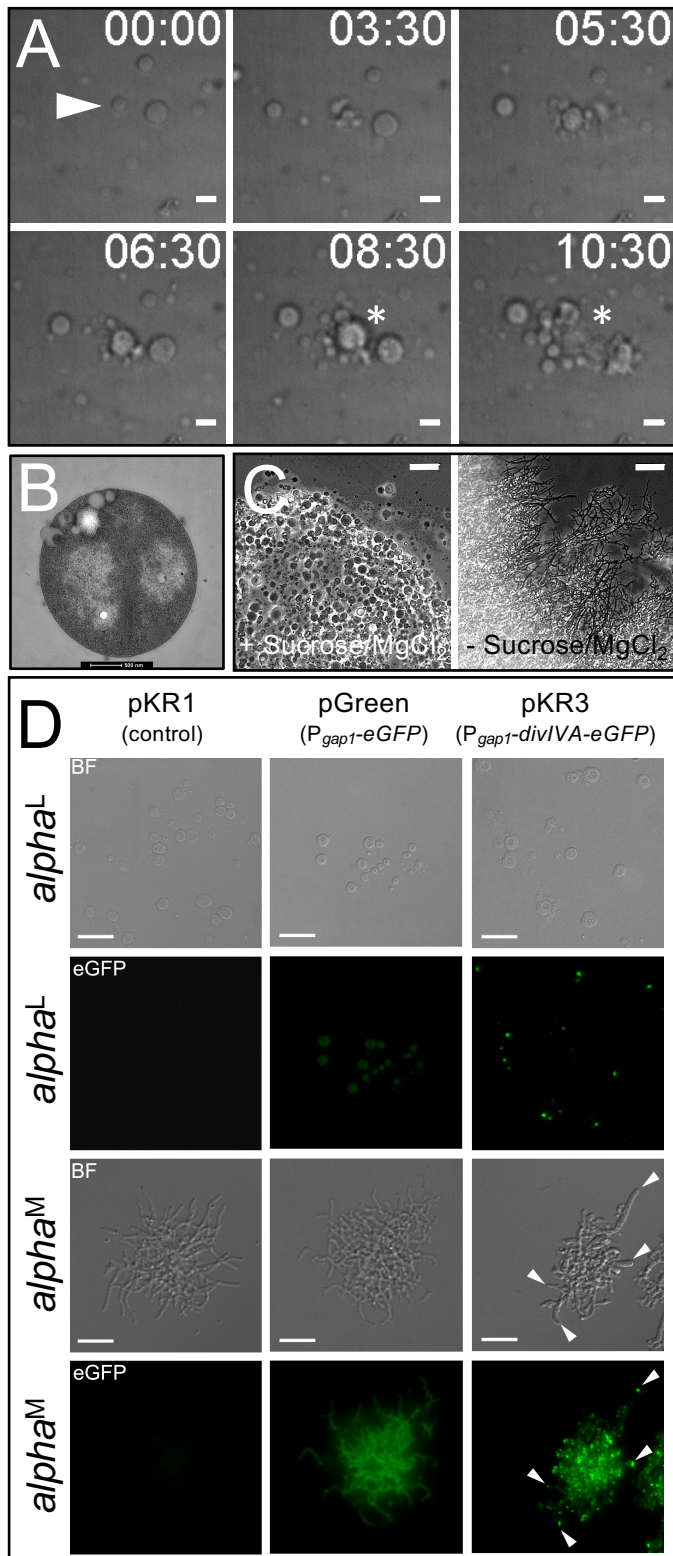


Figure 2. Characterization of the stable L-form cell line *alpha*. (A) Phase-contrast images from Extended Data Video S6, which demonstrate the proliferation of *alpha* in the L-form state. The arrowhead points to the dividing mother cell. Please note that after the generation of new progeny the mother cell lysis (indicated with an asterisk). (B) Transmission electron micrograph showing an *alpha* cell lacking the cell wall. (C) On plates containing sucrose and MgCl₂, *alpha* forms colonies exclusively containing L-forms, while it forms mycelial colonies on plates without these supplements. (D) L-forms of *alpha* (*alpha*^L) transformed with pGreen, leading to the constitutive expression of eGFP, show a diffuse cytosolic GFP signal. By contrast, L-form cells containing pKR3, thereby expressing eGFP fused to DivIVA, show distinct foci localized to the membrane. When the strains are grown as a mycelium (*alpha*^M), DivIVA-eGFP localized to the hyphal tips (arrowheads). No fluorescence is observed in cells or mycelium containing the control plasmid pKR1. Scale bars represent 500 nm (B), 5 μm (A), 10 μm (D) or 20 μm (C).

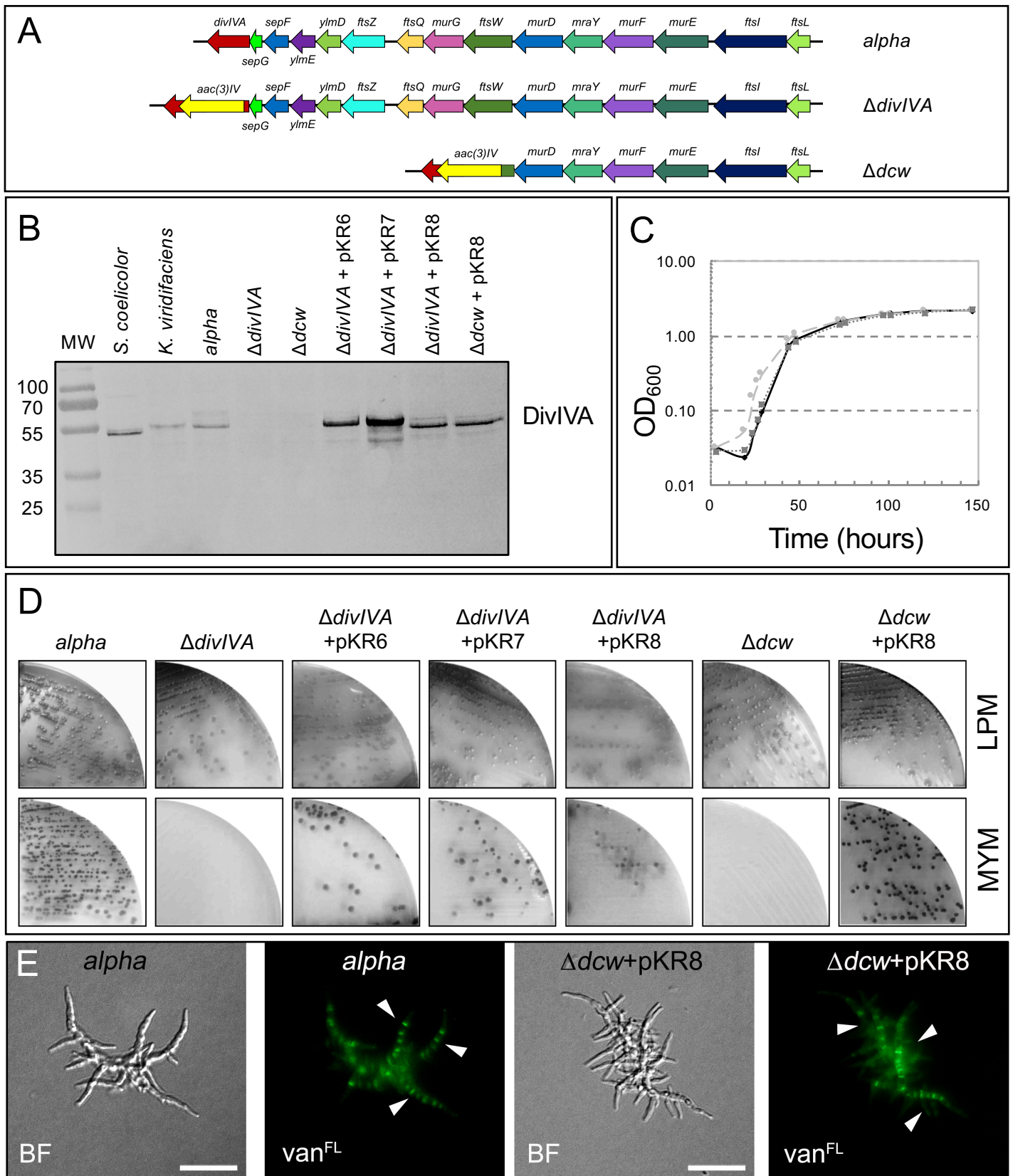
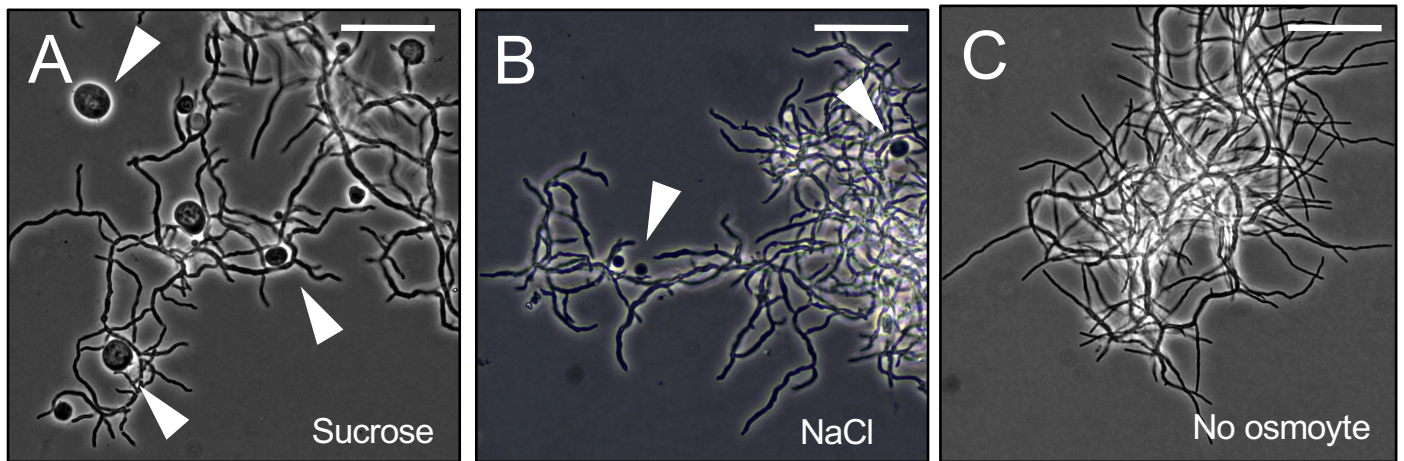
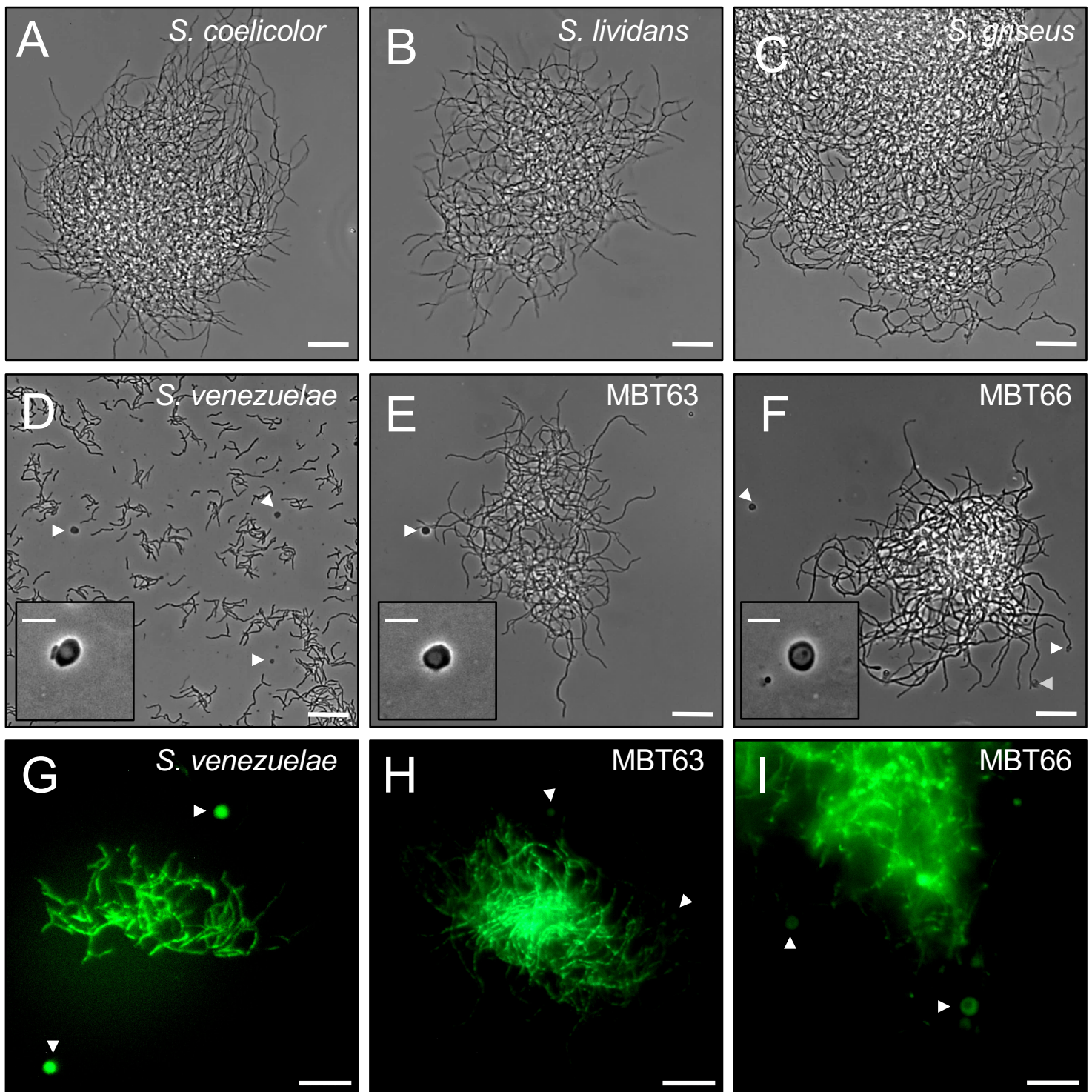


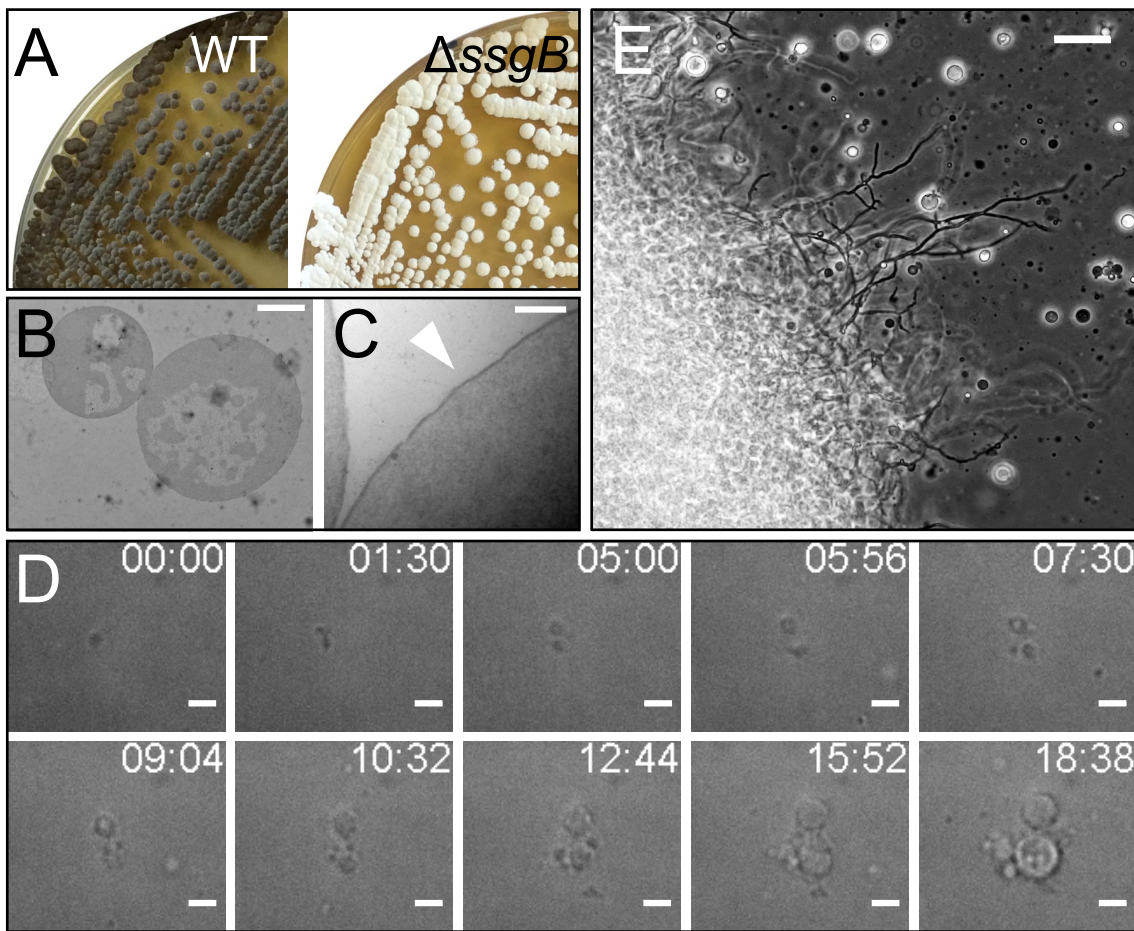
Figure 3. Reversible metamorphosis depends on DivIVA. (A) Illustration of the *dcw* clusters in *alpha* and the derivative strains lacking *divIVA* or part of the *dcw* cluster. (B) Western analysis confirming the absence of DivIVA in the $\Delta divIVA$ and Δdcw mutants. Introduction of *divIVA* under control of its own (pKR6) or the *gap1* (pKR7) promoter restores the presence of DivIVA. Likewise, introduction of the *S. coelicolor dcw* gene cluster (on pKR8) in the $\Delta divIVA$ or Δdcw mutant strains restores the presence of DivIVA. MW is the molecular weight in kDa. (C) Comparable growth between *alpha* (solid black line) and the $\Delta divIVA$ (dashed line) and the Δdcw mutants (dotted line) in liquid LPM medium. (D) The mutant strains lacking *divIVA* can no longer grow on MYM plates lacking sucrose and $MgCl_2$. (D) Reintroduction of the *S. coelicolor dcw* gene cluster (on pKR8) in the Δdcw mutant restores mycelial growth, including septal PG synthesis, as revealed by staining with fluorescent vancomycin (vanFL). Scale bar represents 5 μm .



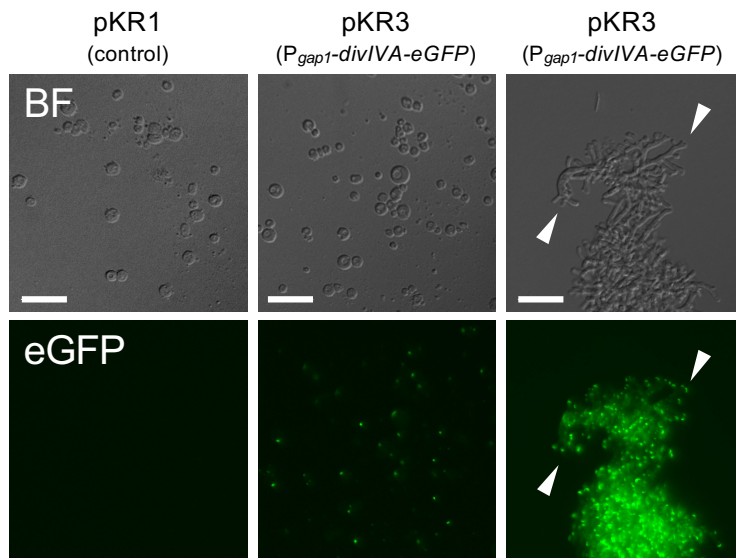
Extended Data Figure S1. Osmolytes are required for the formation of wall-less cells. The addition of 0.6M sucrose (A) or NaCl (B) to LPB medium is required for the formation of wall-less cells. No wall-less cells are detected without the addition of osmolytes (C). Scale bars represent 20 μm .



Extended Data Figure S2. Formation of wall-less cells in *Streptomyces* and *Kitasatospora* species. Unlike *Streptomyces coelicolor* (A), *Streptomyces lividans* (B) and *Streptomyces griseus* (C), wall-less (arrowheads) are evident in *Streptomyces venezuelae* (D), and *Kitasatospora* strains MBT63 (E) and MBT66 (F) grown in LPB medium. The inlays show magnified versions of wall-less cells in these species. (G-I). Visualization of DNA in wall-less cells using SYTO9. Scale bars represent 5 μm (inlays), 10 μm (G-I) or 20 μm (A-F).



Extended Data Figure S3. Reversible metamorphosis in the *K. viridifaciens* $\Delta ssgB$ mutant. (A) Deletion of *ssgB* in *K. viridifaciens* blocks the formation of grey spores. (B, C) Transmission electron micrographs of N-forms of the $\Delta ssgB$ mutant strain indicates that they lack the cell wall. The arrowhead indicates the cell membrane (C). (D) Phase-contrast images from Extended Data Video S5 showing N-form proliferation in liquid medium. The times are indicated in HH:MM. (E) Plating of N-forms of the *ssgB* mutant on LPMA yields colonies consisting of mycelia and N-forms. Scale bars represent 200 nm (C), 2 μ m (B), 10 μ m (D) or 20 μ m (E).



Extended Data Figure S4. Functional complementation of the Δ *divIVA* mutant by DivIVA-eGFP The DivIVA-eGFP fusion expressed from pKR3 restores filamentous growth of the *divIVA* mutant, and localizes to the hyphal tips (arrowheads). Scale bars represent 10 μ m.